Supplementary Figures and Supplementary Table 1

Molecular pathology, developmental changes and synaptic dysfunction in (pre-) symptomatic human C9ORF72-ALS/FTD cerebral organoids

Astrid T. van der Geest[1], Channa E. Jakobs[1], Tijana Ljubikj[1], Christiaan F.M. Huffels[1], Marta Cañizares Luna[1], Renata Vieira de Sá[1], Youri Adolfs[1], Marina de Wit[1], Daan H. Rutten[1], Marthe Kaal[1], Maria M. Zwartkruis[2], Mireia Carcolé[3], Ewout J.N. Groen[2], Elly M. Hol[1], Onur Basak[1], Adrian M. Isaacs[3], Henk-Jan Westeneng[2], Leonard H. van den Berg[2], Jan H. Veldink[2], Domino K. Schlegel[1] and R. Jeroen Pasterkamp[1*]

[1]Department of Translational Neuroscience, UMC Utrecht Brain Center, University Medical Center Utrecht, Utrecht University, Utrecht, The Netherlands.

[2]Department of Neurology and Neurosurgery, UMC Utrecht Brain Center, University Medical Center Utrecht, Utrecht University, Utrecht, The Netherlands.

[3]UK Dementia Research Institute at UCL and Dept. of Neurodegenerative Disease, UCL Queen Square Institute of Neurology, London, United Kingdom

*Correspondence: r.j.pasterkamp@umcutrecht.nl

Supplementary Fig. 1

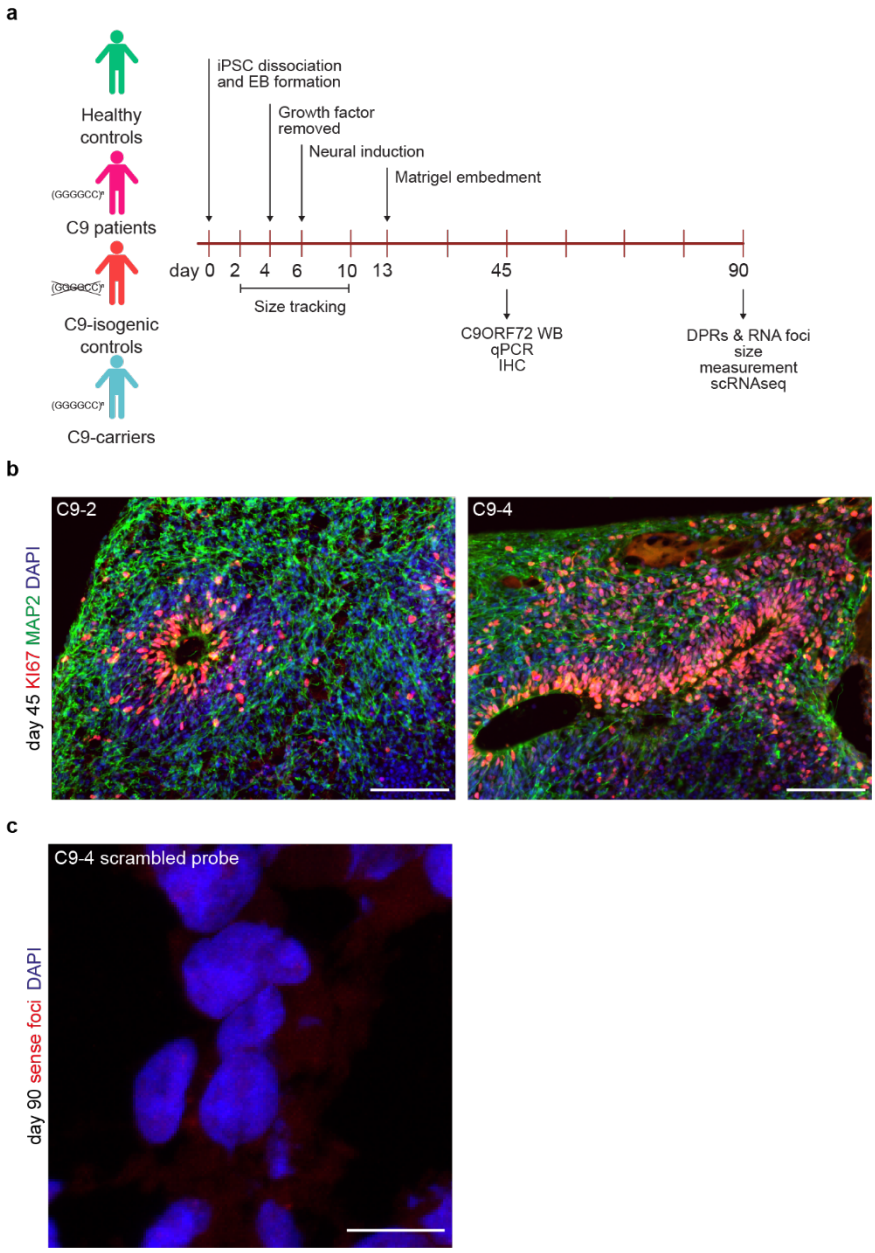

Supplementary Fig. 1 Characterization of C9-ALS/FTD cerebral organoids

a) Schematic overview of the cerebral organoid culture, subjects, and timing of experiments.

b) Representative image of immunohistochemistry on cryosections of day 45 cerebral organoids from C9-ALS/FTD (C9) patients other than shown in **Fig. 1c** for MAP2 (green; neuronal part) and KI67 (red; ventricular zone) in combination with DAPI to mark nuclei.

c) Representative images showing lack of LNA-FISH signal for scrambled control probes (red) in a cryosection of a day 90 C9 organoid. DAPI (blue) marks nuclei.

Scale bar: **b**) 100 µm, **c)** 10 µm.

Supplementary Fig. 2

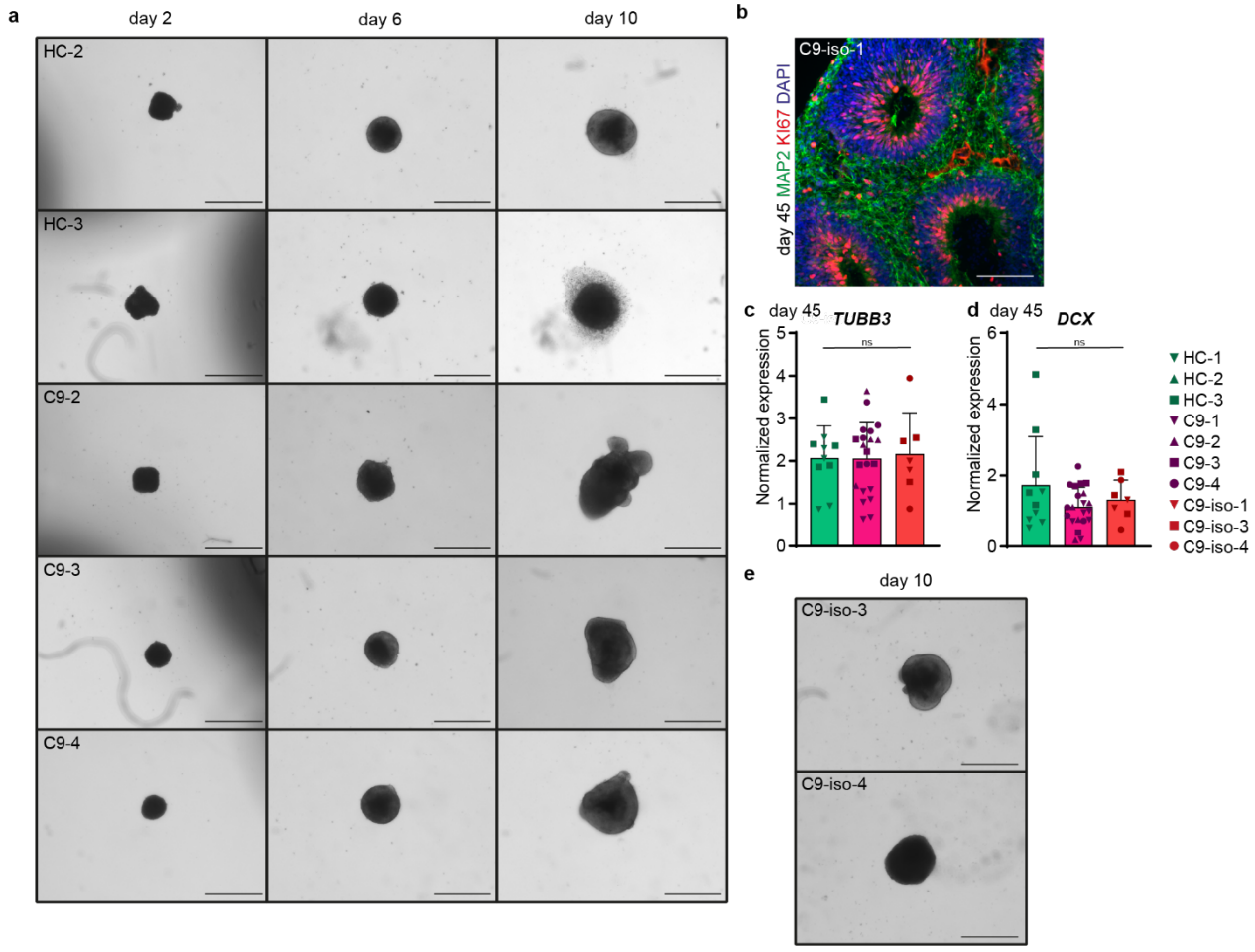

Supplementary Fig. 2 C9-HRE causes early accelerated cerebral organoid growth

a) Representative brightfield images of healthy control (HC) and C9-ALS/FTD (C9) cerebral organoids at day 2, 6, and 10.

b) Representative image of immunohistochemistry on a cryosection of a day 45 cerebral organoids from a C9 isogenic control (C9-iso) for MAP2 (green; neuronal part) and KI67 (red; ventricular zone) in combination with DAPI to mark nuclei.

c, d) Quantitative PCR for the neuronal cytoskeleton marker *TUBB3* and early neuron marker *DCX* in day 45 HC, C9, and C9-iso organoids. Expression is normalized to *TBP* and *RPII*. Data are shown as the mean ± SEM, symbols indicate specific lines and dots represent ≥ 3 pooled organoids. 2-6 independent organoid differentiations were performed per iPSC line. One-way ANOVA, *TUBB3*: $F(2,35) = 0.04231$, $p = 0.9586$; *DCX*: $F(2,35) = 1.844$, $p = 0.09532$.

e) Representative brightfield images of C9-iso organoids at day 10.

Scale bars: **a, e, f)** 500 µm, **b)** 100 µm.

Supplementary Fig. 3

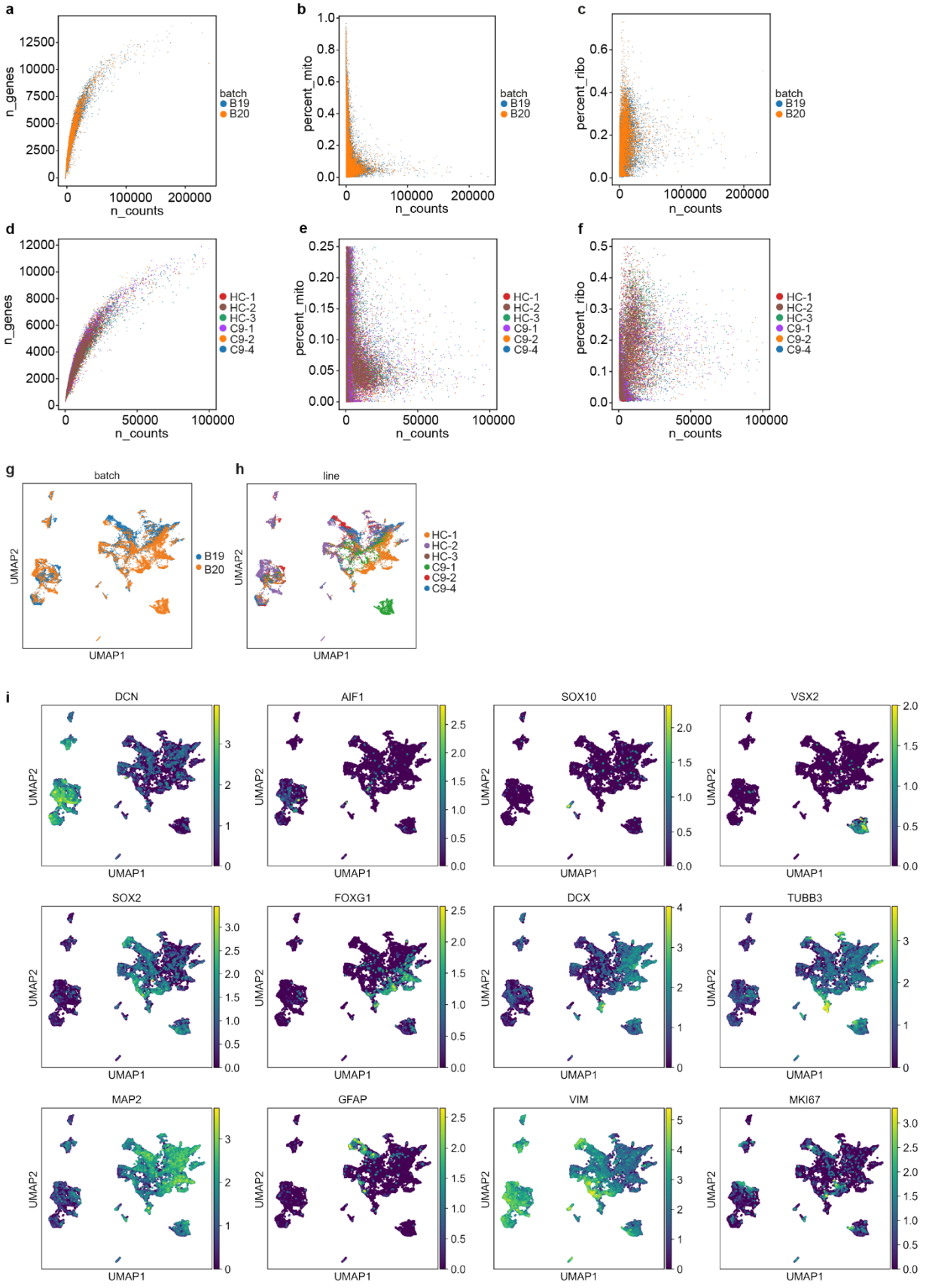

j

Cell type composition day 90 organoids

	HC-1	HC-2	HC-3	C9-1	C9-2	C9-4
(upper layer) neuron	18%	2%	12%	13%	6%	34%
glia/astrocyte	1%	4%	7%	1%	16%	14%
unknown1	6%	2%	11%	17%	11%	5%
non-neuronal/gliogenic	9%	38%	17%	3%	17%	18%
choroid plexus	0%	10%	11%	0%	3%	1%
radial glia/early neuron	24%	0%	3%	8%	0%	0%
unknown2	1%	11%	4%	1%	2%	1%
neuron	24%	7%	5%	4%	13%	5%
radial glia	4%	10%	7%	4%	15%	7%
deep layer neuron	0%	4%	3%	0%	1%	0%
early neuron	5%	3%	5%	3%	5%	7%
glutamatergic excitatory neuron	5%	0%	0%	1%	0%	0%
non-neuronal	2%	5%	11%	2%	8%	4%
GABAergic inhibitory neuron	1%	0%	1%	0%	0%	0%
endothelium	0%	3%	0%	0%	0%	1%
oligodendrocyte precursor cell	0%	1%	2%	0%	1%	2%
retinal pigment epithelium	0%	0%	0%	44%	0%	0%

k

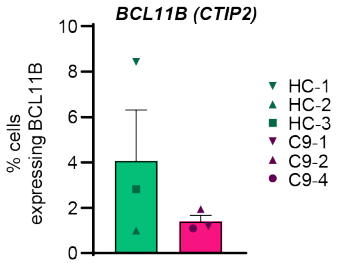

Supplementary Fig. 3 Quality control single-cell RNA sequencing data and cell type abundance data

a-c) Scatter plots showing cells before filtering. Number of read counts per cell is plotted against number of genes (**a**), percentage of mitochondrial reads (**b**), and percentage of ribosomal reads (**c**). Colours indicate the organoid batch (B19 or B20).

d-f) Scatter plots showing cells after filtering. Number of counts per cell is plotted against number of genes (**d**), percentage of mitochondrial reads (**e**), and percentage of ribosomal reads (**f**). Colours indicate the iPSC lines used to generate cerebral organoids. HC, healthy control; C9, C9-ALS/FTD.

g, h) Uniform manifold approximation and projection (UMAP) plot of the filtered and normalized scRNAseq data color-coded by organoid batch (**g**) or iPSC line (**h**).

i) UMAP showing expression of different marker genes for the annotated cell types; *DCN* – gliogenic; *AIF1* – microglia; *SOX10* – OPCs; *VSX2* – retinal epithelium; *SOX2* – stem cells; *FOXG1* – forebrain cells; *DCX* – early neurons; *TUBB3* – neuronal cytoskeleton; *MAP2* – neural soma and dendrites; *GFAP* – astrocytes; *VIM* – radial glia; *MKI67* – proliferative cells.

j) Table displaying cell type abundance in organoids per experimental group separated by annotated clusters.

k) Percentage of cells expressing *BCL11B* (*CTIP2*) in dataset. Graph shows mean ± SEM, symbols indicate specific lines.

Supplementary Fig. 4

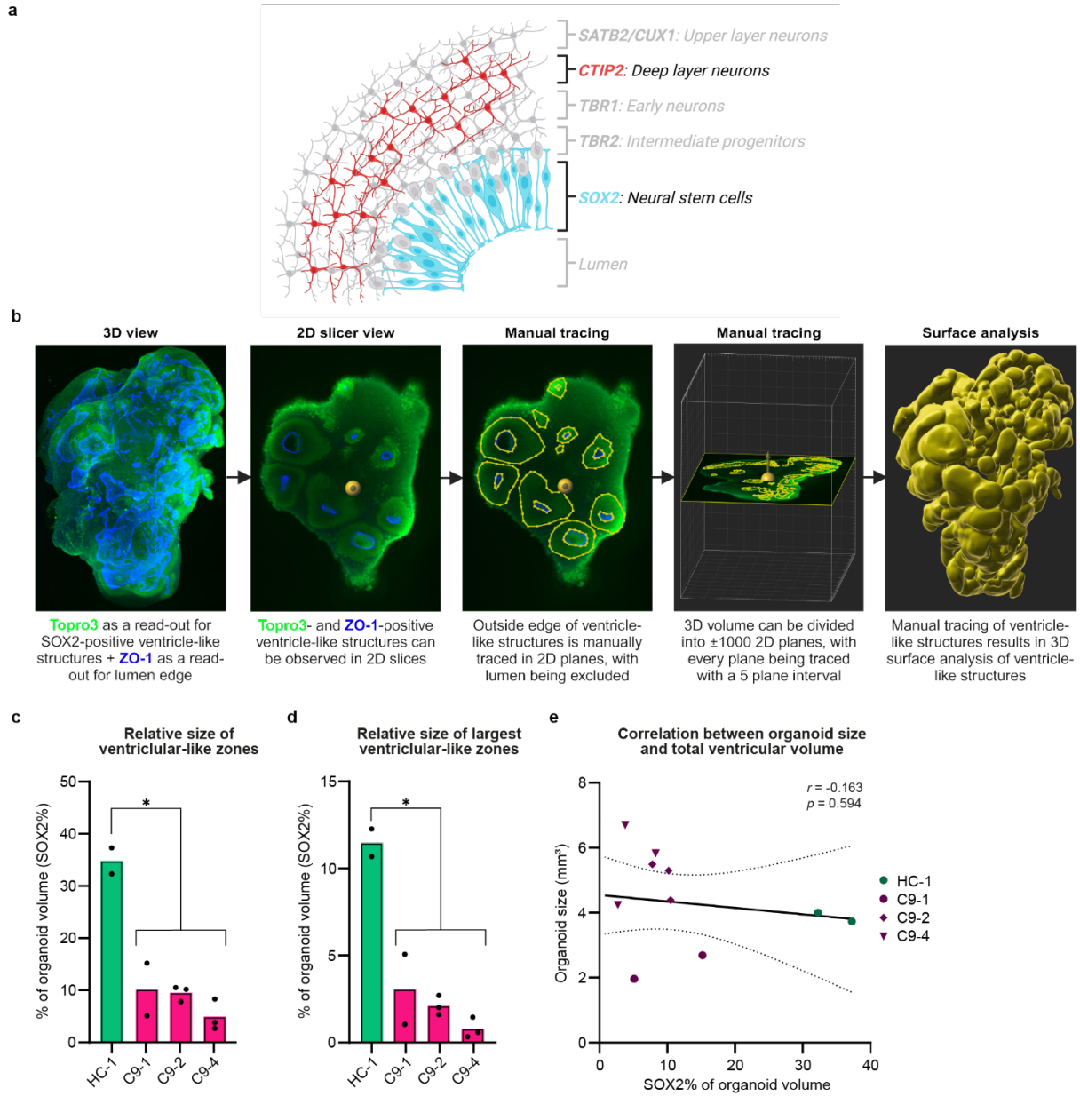

Supplementary Fig. 4 Expression of CTIP2 and SOX2 in (pre)symptomatic C9-HRE cerebral organoids and ventricular zone analysis in cerebral organoids using FLSM

a) Schematic representation of cerebral organoid microstructure, highlighting the location of $SOX2^+$ radial glia/neural stem cells (cyan) lining the ventricular lumen, surrounded by $CTIP2^+$ deep layer neurons (red).

b) Analysis workflow of the Fluorescent Light Sheet Microscopy (FLSM) experiments on day 90 cerebral organoids stained with TOPRO3 to highlight the denser ventricular-like zones (VLZs) in green, which was confirmed by the stem cell marker SOX2. The tight junction marker ZO-1 stained the edge of the ventricular lumen. Manual tracing was performed with a 5-plane interval to create 3D volumes of VLZs.

c) Volume of summation of all VLZs relative to organoid volume of every analysed organoid, separated by experimental group (iPSC line). Graph shows individual organoids measured (n= 2-3 organoids per line for 1 HC and 3 C9 lines), statistical comparison between disease conditions: Mann-Whitney Test, U = 0, $p = 0.0444$.

d) Volume of the 3 largest VLZs relative to organoid volume of every analysed organoid. Graph shows individual organoids measured (n= 2-3 organoids per line for 1 HC and 3 C9 lines), statistical comparison between disease conditions: Mann-Whitney Test, U = 0, $p = 0.0444$.

e) Scatterplot depicting the relation between total organoid volume and relative volume of VLZs in every organoid. Symbols indicate experimental group (iPSC line). The line indicated the correlation fitted to these data points, Pearson's correlation $r(11) = -0.163$, $p = 0.594$. HC-1 was used as a representative control (**b-d**).

* = $p < 0.05$.

Supplementary Fig. 5

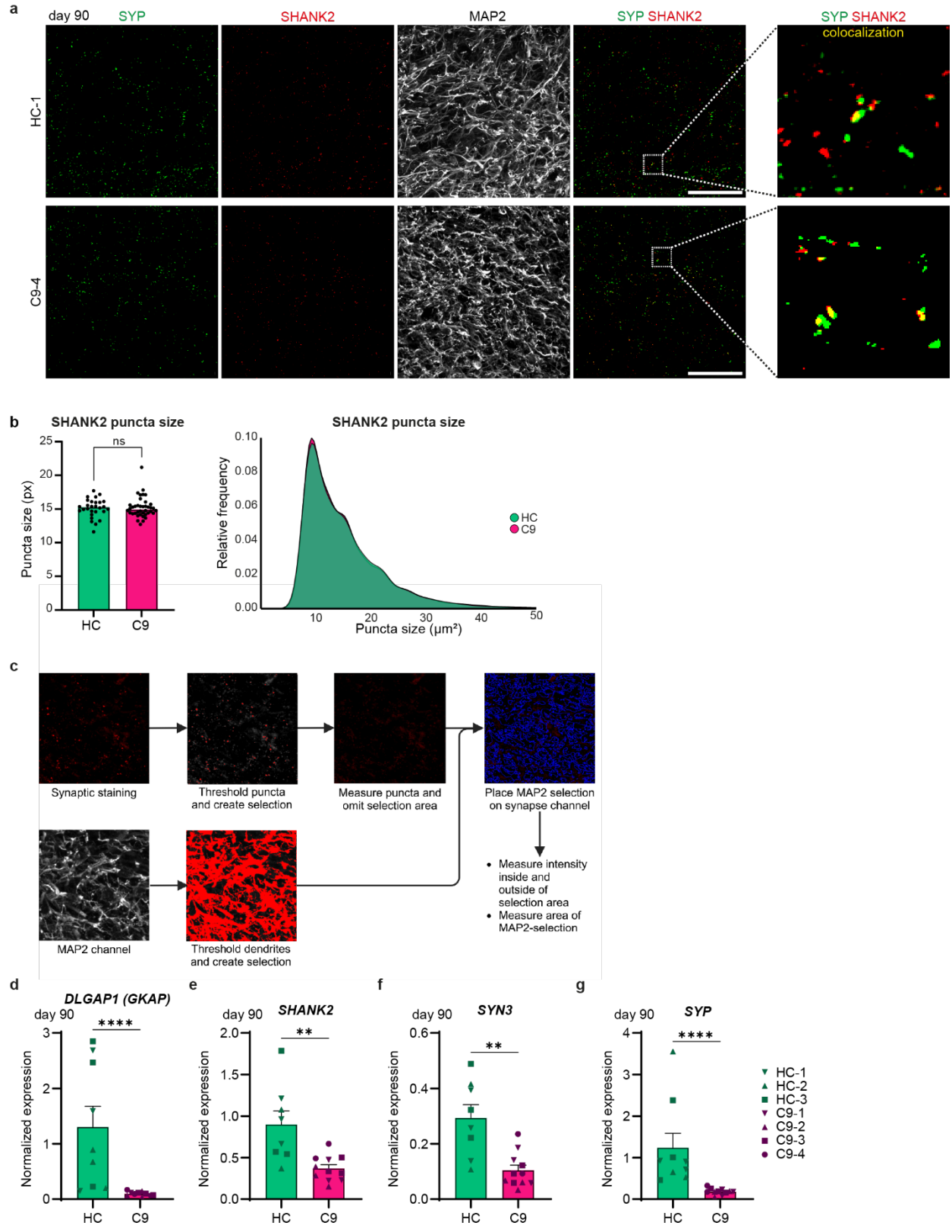

Supplementary Fig. 5 Glutamatergic synapse analysis in day 90 cerebral organoids

a) Immunohistochemistry to visualize glutamatergic synapses for the presynaptic marker synaptophysin (SYP; green), the postsynaptic marker SHANK2 (red), and MAP2, to label dendrites (white) in day 90 HC and C9 organoids. Boxed regions are shown at higher magnification on the right (co-localization of SYN and SHANK2). Quantifications in **Fig. 5b-f** derive from images as in **a**.

b) Size of SHANK2 puncta averaged per image (left) and relative size frequency of individual puncta (right). Graph shows mean, dots represent mean of one image, images were taken from three organoids from 2-3 independent differentiations (n=3 healthy control (HC), n=4 C9-ALS/FTD (C9) lines). Unpaired T-test, $t(66) = 0.2443$, $p = 0.8078$

c) Analysis workflow used to determine puncta intensity and signal intensity in $MAP2^+$ dendrites. The dendritic region of interest was defined by thresholding MAP2 staining measurements.

d-g) Quantitative PCR was performed for glutamatergic synaptic genes and major synaptic components in day 90 healthy control (HC) and C9-ALS/FTD (C9) organoids as an extension of **Fig. 5g-k**. Expression was normalized to the housekeeping genes *TBP* and *RPII*. Graphs show mean ± SEM, symbols indicate the cell lines, dots represent an average measurement of 3 organoids pooled per independent organoid induction (n=4 C9, and n=3 HC lines). Mann-Whitney two-tailed t-test, *DLGAP1*: $U(18) = 1$, $p < 0.0001$; *SHANK2*: $U(18) = 8$, $p = 0.0018$; *SYN3*: $U(18) = 1$, $p = 0.0018$; *SYP*: $U(19) = 0$, $p < 0.0001$.

Scale bar: **a**) 40 µm. ** = $p < 0.01$. **** = $p < 0.0001$.

Supplementary Fig. 6

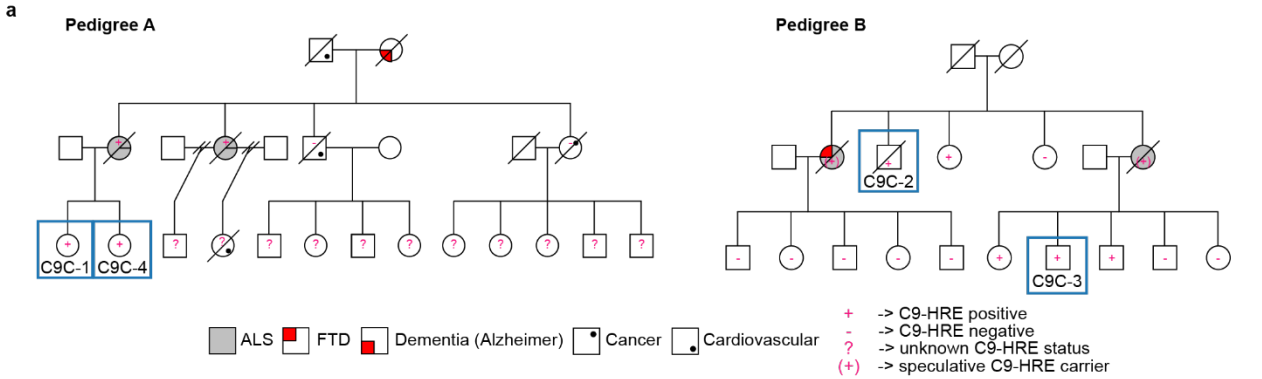

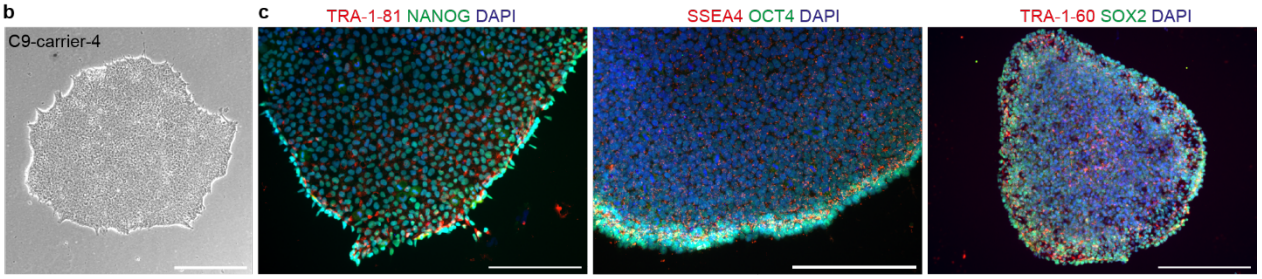

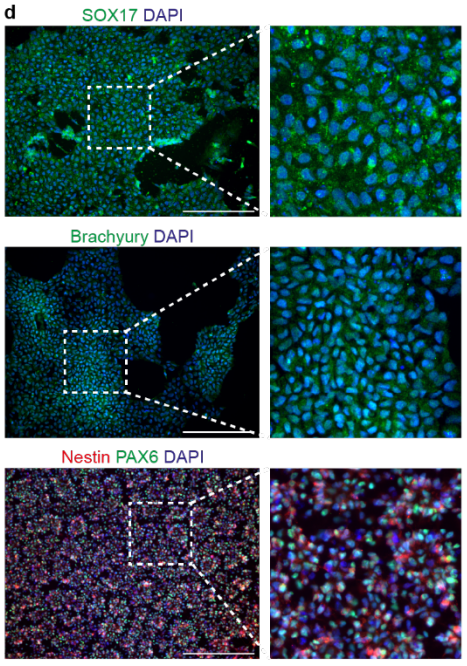

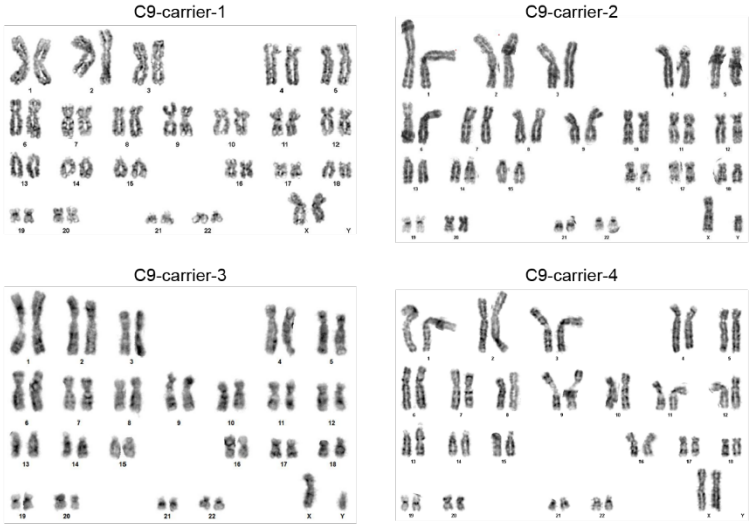

f **Karyotype summary**

C9-carrier	1	2	3	4
% corresponding to indicated karyotype	46 XX (90%)	46 XY (85%)	46 XY (95%)	46 XX (80%)

g **Fibroblast-iPSC identity match**

C9-carrier	1	2	3	4
% corresponding to fibroblast	100%	100%	100%	100%

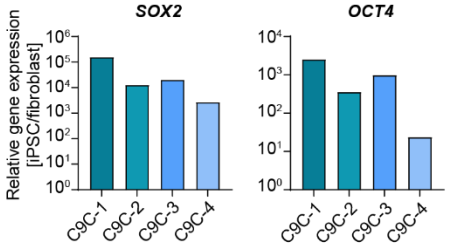

Supplementary Fig. 6 Characterization of cerebral organoids from presymptomatic C9-HRE carriers

a) Pedigrees of C9-HRE carriers used in this study. Individuals from whom lines were derived are indicated by blue squares and the corresponding line name. In Pedigree A, the mother of C9-carrier-1 (C9C-1) and C9C-4 had C9-ALS and survived for 2.5 years after symptom onset. One aunt of these carriers survived C9-ALS for only 1.25 years after symptom onset. Another aunt and uncle were C9-HRE-negative and died of other causes. The grandmother had dementia and the grandfather died from cardiovascular causes. In F1 of pedigree B, four out of five siblings are (predicted to be) C9-HRE-positive. C9C-2 was part of the F1 generation but died at the age of 40 because of causes other than ALS or FTD. Two sisters of C9C-2 had C9-ALS of which one sister was additionally diagnosed with FTD. The sister with C9-ALS is the mother of C9C-3, who survived for 4 years after symptom onset. Among C9C-3s five siblings, three were determined to be C9-HRE-positive. The other sister with C9-ALS/FTD, had five children who were all determined to be C9-HRE-negative. This sister passed away at the age of 43.

b) Representative brightfield image of an iPSC colony after Sendai reprogramming. C9-carrier-4 is displayed.

c) Representative images of immunohistochemistry on iPSCs for the pluripotency markers TRA-1-81, NANOG, SSEA4, OCT4, TRA-1-60 and SOX2. C9-carrier-4 is displayed.

d) Representative images of immunohistochemistry on iPSCs differentiated into three germ layers to demonstrate pluripotency potential. SOX17 marks endoderm, Brachyury marks mesoderm, Nestin and PAX6 mark ectoderm. C9-carrier-4 is displayed. Boxed area is shown at higher magnification on the right.

e, f) Characterization of DNA integrity, **e)** representative images of karyograms of iPSC lines from C9-carriers and **f)** karyotyping summary over 20 independent characterisations per iPSC line.

g) Summary Table of fibroblast-iPSC identity matching using short tandem repeat (STR) analysis. **h)** Quantitative PCR for the pluripotency markers *SOX2* and *OCT4* in iPSCs from all four C9-carriers. Bars display a ratio of expression in iPSCs compared to the related fibroblasts, ratio is the average of two technical replicates per sample.

Scale bars: **b)** 400 µm, **c, d)** 200 µm.

Supplementary Fig. 7

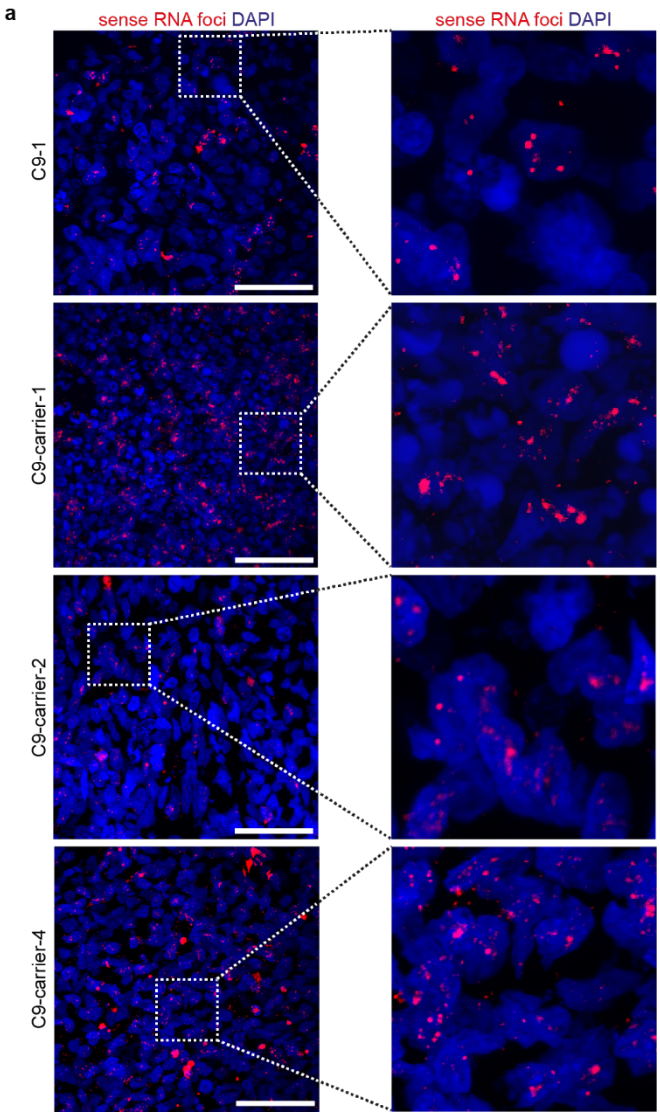

Supplementary Fig. 7 Cerebral organoids from presymptomatic C9-HRE carriers display sense RNA foci from C9-HRE

a) Representative images showing LNA-FISH for sense RNA foci (red) in cryosections of day 90 C9-carrier organoids. DAPI (blue) marks nuclei. Boxed areas are shown at higher magnification at the right. Scrambled control probes did not result in specific signal (example displayed in **Fig. 7f**). Scale bars: **a)** 50 µm. Higher magnification area is 40 by 40 µm.

Supplementary Fig. 8

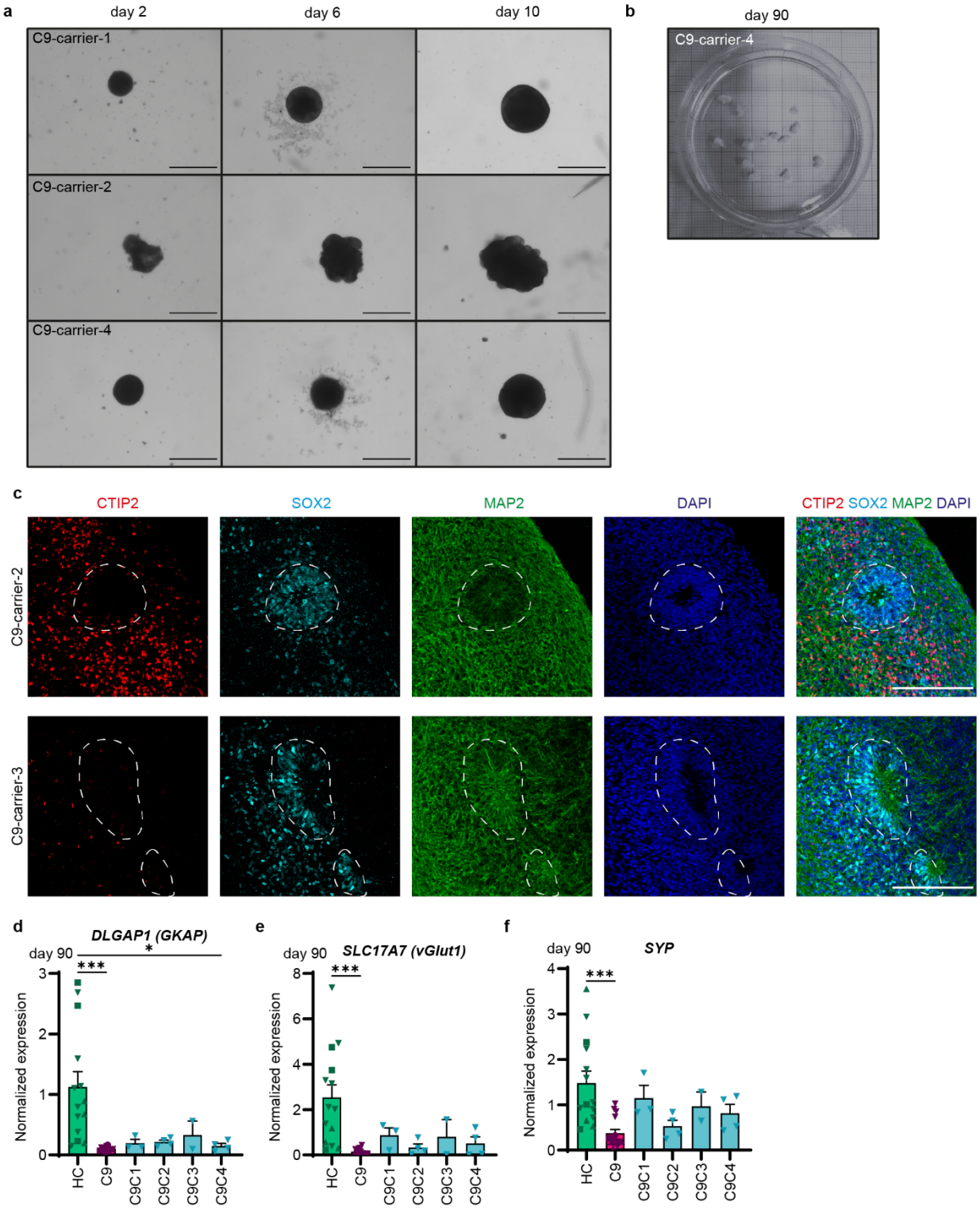

Supplementary Fig. 8 Cerebral organoids from presymptomatic C9-carriers display phenotypes as observed in C9 organoids

a) Representative brightfield images of C9-carrier organoids at day 2, 6, and 10.

b) Representative brightfield image of C9-carrier organoids at day 90.

c) Representative images of immunohistochemistry on a cryosection of day 90 cerebral organoids from C9-carriers as an extension of **Fig. 8f** for CTIP2 (red; deep layer neuron), SOX2 (cyan; neural stem cells marking ventricular-like zone (VLZ)) and MAP2 (green; dendritic network) in combination with DAPI to mark nuclei.

d-f) Quantitative PCR for glutamatergic synaptic genes and major synaptic components in day 90 healthy control (HC), C9-ALS/FTD (C9), and C9-carrier organoids as an extension of **Fig. 8g-m**. Expression was normalized to the housekeeping genes *TBP* and *RPII*. Graphs show mean, dots represent an average measurement of 3 organoids pooled per independent organoid induction (n=4 C9-carrier, n=4 C9, and n=3 HC lines). One-way ANOVA, Tukey's multiple comparisons test, *DLGAP1*: $F(5, 35) = 5.461$, $p = 0.0008$; *SCL17A7*: $F(5, 35) = 5.124$, $p = 0.0013$; *SYP*: $F(5, 36) = 4.653$, $p = 0.0022$.

Scale bar: **a)** 500 µm, **b)** on millimetre paper, **c**) 150 µm.

Supplementary Fig. 9

a

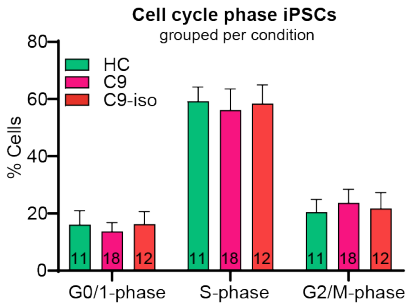

Supplementary Fig. 9 Cell cycle analysis in iPSCs from C9-ALS/FTD patients

a) Quantification showing the percentage of iPSCs in different phases of the cell cycle, grouped per condition. 10.000 cells were quantified per experiment over 5 independent experiments (n=3 HC, 4 C9, 3 C9-iso). Graph shows mean ± SEM. Two-way ANOVA, $F(2,114) = 0.39$, $p = 0.6787$.

Supplementary Table 1 - iPSC lines

used in this study

Condition	Name in lab	Name in paper	Gender	Age at sampling	C9-repeat size*		Reference
					allele 1	allele 2	
HC	929c4	HC-1	Female	60	2	7	made at UMC Utrecht Brain Center MIND facility (manuscript in submission)
HC	OH2.6	HC-2	Male	61	5	5	Harschnitz et al. (Annals of neurology, 2016); Ormel & Vieira de Sá et al., (Nature Communications, 2018); called iPSC2
HC	OH4.6	HC-3	Female	60	2	2	made at UMC Utrecht Brain Center MIND facility (manuscript in revision)
C9	6769	C9-1	Female	46	13	961	Shi et al. (Nature Medicine, 2018); https://www.coriell.org/0/Sections/Search/Sample_Detail.aspx?Ref=ND06769
C9-iso	CL1 (ISO_CTRL 6769)	C9-iso-1	Female	46	0	0	Hung et al. (Cell, 2023); Hendricks et al. (Cell Reports, 2023)
C9	12099	C9-2	Male	49	2	809	Shi et al. (Nature Medicine, 2018); https://www.coriell.org/0/Sections/Search/Sample_Detail.aspx?Ref=ND12099
C9	CS29iALS-C9n1	C9-3	Male	47	2	1175	https://biomanufacturing.cedars-sinai.org/product/cs29ials-c9nxx/ ; Sareen et al. (Science Translational Medicine, 2013)
C9-iso	CS29iALS-C9n1.ISOT2RB4	C9-iso-3	Male	47	0	0	https://biomanufacturing.cedars-sinai.org/product/cs29ials-c9n1-isoxx/
C9	CS52iALS-C9n6	C9-4	Male	57	2	886	https://biomanufacturing.cedars-sinai.org/product/cs52ials-c9nxx/ ; Sareen et al. (Science Translational Medicine, 2013)
C9-iso	CS52iALS-C9n6.ISOC3	C9-iso-4	Male	57	0	0	https://biomanufacturing.cedars-sinai.org/product/cs52ials-c9n6-isoxx/

C9-carrier	C9C1	C9-carrier-1	Female	44	4	896	made at UMC Utrecht Brain Center MIND facility (this publication)
C9-carrier	C9C2	C9-carrier-2	Male	54	4	871.5	made at UMC Utrecht Brain Center MIND facility (this publication)
C9-carrier	C9C3	C9-carrier-3	Male	29	2	998	made at UMC Utrecht Brain Center MIND facility (this publication)
C9-carrier	C9C4	C9-carrier-4	Female	42	5	666	made at UMC Utrecht Brain Center MIND facility (this publication)
TDP43	TDP0102-M337V	TDP43-1	Male	61	undertermined	undertermined	Dafinca et al. (Stem Cell Reports, 2020)
TDP43	TDP0304-I383T	TDP43-2	Male	58	undertermined	undertermined	Dafinca et al. (Stem Cell Reports, 2020)
ATXN2	A18	ATXN2-1	Male	72	undertermined	undertermined	made at UMC Utrecht Brain Center MIND facility (manuscript in revision)
ATXN2	B11	ATXN2-2	Male	74	undertermined	undertermined	made at UMC Utrecht Brain Center MIND facility (manuscript in revision)
ATXN2	GG1	ATXN2-3	Male	77	undertermined	undertermined	made at UMC Utrecht Brain Center MIND facility (manuscript in revision)
ATXN2	N9	ATXN2-4	Female	38	undertermined	undertermined	made at UMC Utrecht Brain Center MIND facility (manuscript in revision)
ATXN2	P1	ATXN2-5	Male	55	undertermined	undertermined	made at UMC Utrecht Brain Center MIND facility (manuscript in revision)

* determined by RP-PCR for repeats under 30. For repeats over 30 median length is displayed